ECOLOGY LETTERS

Ecology Letters, (2015) doi: 10.1111/ele.12521

LETTER

Imperfect prey selectivity of predators promotes biodiversity and irregularity in food webs

Alexey B. Ryabov,[1]* Andrew Morozov,[2] and Bernd Blasius[1]

[1]*University of Oldenburg Institute for Chemistry and Biology of the Marine Environment (ICBM) Oldenburg, Germany*
[2]*Department of Mathematics University of Leicester Leicester, UK; Shirshov Institute of Oceanology, RAS, Moscow, Russia*

**Correspondence: E-mail: alexey.ryabov@uni-oldenburg.de*

Abstract

Ecological communities are often characterised by many species occupying the same trophic level and competing over a small number of vital resources. The mechanisms maintaining high biodiversity in such systems are still poorly understood. Here, we revisit the role of prey selectivity by generalist predators in promoting biodiversity. We consider a generic tri-trophic food web, consisting of a single limiting resource, a large number of primary producers and a generalist predator. We suggest a framework to describe the predator functional response, combining food selectivity for distinctly different functional prey groups with proportion-based consumption of similar prey species. Our simulations reveal that intermediate levels of prey selectivity can explain a high species richness, functional biodiversity, and variability among prey species. In contrast, perfect food selectivity or purely proportion-based food consumption leads to a collapse of prey functional biodiversity. Our results are in agreement with empirical phytoplankton rank-abundance curves in lakes.

Keywords

Biodiversity, coexistence, ecosystem productivity, multi-prey functional response, paradox of plankton.

Ecology Letters (2015)

INTRODUCTION

Revealing the mechanisms which account for the high biodiversity observed in nature remains one of the most crucial ecological challenges (Tilman 1982; Kondoh 2003; Ives & Carpenter 2007). Several mechanisms have been suggested to resolve the famous 'paradox of plankton' – the coexistence of many phytoplankton species competing over a few vital resources in an apparently homogeneous environment (Hutchinson 1961). These include spatial and temporal heterogeneity of the environment, environmental fluctuations, non-equilibrium intrinsic dynamics, and non-competitive interactions with other species (Huisman *et al*. 2001; Amarasekare 2003; Scheffer *et al*. 2003; Roy & Chattopadhyay 2007; Ryabov & Blasius 2011).

A body of empirical evidence suggests that predation pressure on competing species occupying the same trophic level can play an important role in promoting biodiversity (Risch & Carroll 1982; Proulx *et al*. 1996; Koen-Alonso & Yodzis 2005). These observations, however, are not fully reflected in ecological theory. Most conceptual models assume that food consumption is non-selective and determined by the relative abundances of prey species, in which case one predator can mediate the coexistence of maximally two prey species sharing a single resource (Holt *et al*. 1994; Leibold 1996). Even in complex 3D ocean marine ecosystem models which incorporate both spatial and temporal heterogeneity, the number of locally coexisting phytoplankton species under proportion-based grazing by zooplankton typically does not exceed three (Follows *et al*. 2007).

This discrepancy can be resolved by assuming food selectivity, or active switching, between multiple prey species (Murdoch 1969). Prey selectivity means that a predator can adaptively adjust its preference for more abundant or more profitable prey, which can arise due to several generic mechanisms. For instance, the consumption of a particular type of prey might require specific strategies or some acclimation time to produce specific digestion ferments (Murdoch 1969; Allen 1988; Kiørboe *et al*. 1996; Gentleman *et al*. 2003; Loeuille 2010). Prey selectivity can enhance species coexistence and food web stability (Roughgarden & Feldman 1975; Hutson 1984; Kondoh 2003; Prowe *et al*. 2012a,b) since the predation pressure on highly abundant competitors disproportionally increases with their population density, thus providing a virtual refuge for weaker competitors (Hambäck 1998; Abrams & Matsuda 2003).

The concept of prey selectivity has been experimentally established for rather small communities and it is not immediately obvious how to scale it up to diverse communities with hundreds of interacting species. The key problem is an appropriate description of the multi-prey functional response of a generalist predator exhibiting food selectivity behaviour (Gentleman *et al*. 2003). A thorough analysis shows that most functional forms which have been proposed in the literature may not be applicable when the number of resources is large (Morozov & Petrovskii 2013). These standard formulations of the functional response assume that the ability of a predator to distinguish between different prey species is independent of the overall number of species. In contrast, here we propose that prey species form functional groups. A predator can only distinguish the species between groups, but has a limited ability to distinguish the species within a group since they are morphologically close. Consequently, the rate at which a prey species is consumed is determined not only by the relative abundance (proportion) of this particular species, but also by the relative abundances of conspecifics with close life traits.

To capture this mechanism we implement a transitional type of functional response with *imperfect prey selectivity,* which combines food selectivity of distinctly different prey species and proportion-based consumption of similar prey (van Leeuwen *et al.* 2013; Morozov & Petrovskii 2013). The implementation of this idea has profound consequences for the prey community composition and can resolve discrepancies between ecological theory and field observations.

We assess the role of imperfect prey selectivity in a generic tri-trophic planktonic system, consisting of a single limiting resource, a large number of primary producers and a generalist predator. Using this system as a paradigm of multi-species communities, we show that imperfect food selectivity allows the maintenance of realistic biodiversity patterns and ecosystem functions, which would not be observable in the context of proportion-based consumption. In particular, we show that an intermediate imperfectness in prey selectivity (1) leads to maximal species richness in the prey guild; (2) is crucial for providing high functional biodiversity (whereas perfect selectivity results in the survival of a single prey group with low resource requirements); (3) gives rise to an irregular structure in the biomass distribution across life traits of prey; (4) has a strong impact on the relaxation time of the community; (5) leads to hump-shaped diversity-productivity relationships, and (6) is able to produce rank-abundance distributions that conform to empirical observations. Our proposed framework is general and should be applicable a wide range of prey–predator systems.

METHODS

Functional response of a generalist predator with imperfect selectivity

Consider a generalist predator feeding on a number of prey species $i = 1, \ldots, n$ with densities P_i. The standard approach to quantify the predator intake rate of prey P_i suggests that

$$f_i = \frac{a_i \rho_i P_i}{1 + \sum_k a_k \rho_k h_k P_k} \tag{1}$$

where ρ_i describes the predator preference, a_i is the attack rate, and h_i the handling time for prey species i. This functional response can be obtained in various ecological scenarios (Koen-Alonso & Yodzis 2005). Most studies assume a constant value of ρ_i for each prey species, independent of the abundance of the others. In this case expression (1) yields the so-called *proportion-based functional response* (Gentleman *et al.* 2003). However, in general ρ_i can be functions of prey densities.

An increasing body of empirical and theoretical evidence suggests that many predators (e.g. zooplankton, fish, birds) exhibit pronounced food selectivity towards more abundant prey (Greenwood and Elton, 1979; Allen 1988; Hughes & Croy 1993; Kiørboe *et al.* 1996; Strom & Loukos 1998; Elliott 2006; Bond 2007; Saha *et al.* 2010; Smout *et al.* 2010). Such frequency-dependent predation can be modelled according to the idea of Koen-Alonso & Yodzis (2005): the predator preference dynamically changes to increase the intake of more abundant species so that the preference for prey species i is proportional to its relative biomass

$$\rho_i = \frac{\eta_i P_i}{\sum_j \eta_j P_j} \tag{2}$$

where the η_i describe the density-independent preferences of the predator for prey species i. We will refer to approach (1,2) as the *perfect prey selectivity* of the predator.

Nonetheless, perfect selectivity is an unrealistic assumption in communities with a broad resource spectrum (Morozov & Petrovskii 2013). Perfect selectivity implies that the predator needs a unique strategy for every single prey species it catches, which reduces its ability to consume any other prey species. As a consequence perfect prey selectivity yields a strong dilution effect, i.e. the reduction in feeding rates with prey richness. Assume for simplicity that all prey are characterised by the same values a, h, and η and the total prey biomass P is uniformly distributed among n species, so that $P_i = P/n$. In the case of perfect prey selectivity (2) we obtain $\rho_i = 1/n$ and the total intake rate

$$f = \sum_i f_i = \frac{aP/n}{1 + ahP/n} \tag{3}$$

equals the intake rate of a predator which either feeds on 1/n of the prey population or has an n times lower attack rate (see further detail in online Appendix S6).

In reality, the possible number of predator hunting strategies will typically be much smaller than the number of potential prey. To overcome these problems, we propose that the preference to feed on a particular species should depend on the relative abundance of closely related species. Namely, we define the dynamic preference for prey species i as

$$\rho_i = \frac{\sum_j \eta_j \varepsilon_{ij} P_j}{\sum_j \eta_j P_j} \tag{4}$$

Here, the weight coefficients $\varepsilon_{ij} \epsilon [0, 1]$ describe the pairwise similarities between prey species i and j in terms of the predator's ability to consume prey j when it searches for prey i. The similarity is close to one if feeding on this species requires the same strategy and it is close to zero if feeding requires distinctly different strategies. We also postulate that $\varepsilon_{ii} = 1$. Substituting (4) into (1) we obtain the functional response with *imperfect prey selectivity*.

This framework of imperfect prey selectivity interpolates the previous two functional responses: If all prey species are similar ($\varepsilon_{ij} = 1$) then $\rho_i = 1$ and we obtain the proportion-based response. In contrast, when the consumption of each single prey species requires a unique strategy, then $\varepsilon_{ij} = 0 (i \neq j)$, the ρ_i are given by (2), and we obtain a perfect switching response. In between these two extreme scenarios imperfect prey selectivity (4) yields a transitional functional response. A nearly identical functional response was mechanistically derived by van Leeuwen *et al.* (2013) under the assumption that a predator prefers to feed on species which are similar to previously consumed prey. If the handling times are independent from previous prey, this response corresponds to (1) and

(4) for the case that the density-independent preferences are proportional to the attack rates, $\eta_i \sim a_i$.

The similarity of prey species, ε_{ij}, can correlate with any morphological or biological trait of the prey. We, therefore, associate every prey species with its position in trait space and define the similarity ε_{ij} as a decaying function of the difference in life traits. In the main text we assume that the similarity decays exponentially with the trait difference as

$$\varepsilon_{ij} = \exp\left(-\frac{|H_i - H_j|}{\sigma}\right) \tag{5}$$

where H_i is a life trait (specified below) and the key parameter σ characterises the degree of imperfectness in the food selectivity of the predator. In the extreme case of $\sigma_i = 0$, all $\varepsilon_{ij} = 0 (i \neq j)$, and for large $\sigma_i (\sigma \gg 1)$, we find that all $\varepsilon_{ij} \to 1$. Note that our main results are generally independent of the shape of the decaying function in (5), for instance, we obtain similar findings when the ε_{ij} are described by a Gaussian function of the trait differences (see Appendix S5).

The food web model

We consider a standard tri-trophic food chain in which a generalist predator of density Z feeds on a number of prey species with densities $P_j (j = 1, \ldots, n)$, which in turn compete for a single limiting resource of density N

$$\frac{dN}{dt} = D(N_0 - N) - \alpha \sum_j r_j(N) P_j \tag{6}$$

$$\frac{dP_j}{dt} = P_j\left(r_j(N) - m\right) - f_j(\vec{P}) Z \tag{7}$$

$$\frac{dZ}{dt} = Z\left(\theta \sum_j f_j(\vec{P}) - m_Z\right) \tag{8}$$

Here, N_0 is the equilibrium concentration of the resource in the absence of prey, D is the resource supply rate, α is the amount of the limiting nutrient consumed to produce a unit of prey biomass, m is the prey mortality rate, r_j the growth rate of prey j, θ is the food efficiency and m_Z is the mortality of the predator.

The growth rate of each prey species j is described by standard Monod kinetics (Monod 1950)

$$r_j(N) = \mu \frac{N}{N + H_j} \tag{9}$$

where μ is the maximal growth rate and H_j is the half-saturation constant. From the condition $r_j(N) = m_j$ we obtain the critical resource requirement R_j^* for a monoculture of prey species J, growing in the absence of the predator (Tilman 1982)

$$R_j^* = H_j \frac{m}{\mu - m} \tag{10}$$

The critical resource requirements are an important physiological characteristic: different functional groups typically possess different resource requirements (Litchman *et al.* 2007). In the case of phytoplankton, cell size – one of the most important morphological characteristics – correlates with species competitive ability for resource acquisition (Edwards *et al.* 2011). Consequently, it is reasonable to assume that species which occupy close ecological niches also possess close resource requirements, which is expressed in our model by the assumption that the similarity of prey species is associated with their half-saturation constants, H_i.

The predator ingestion rate is given by the functional response of imperfect prey selectivity, eqns (1), (4) and (5). In addition, we assume a linear trade-off between the predator attack rate a and the resource requirements H_i of the prey (i.e. prey species may invest either in resource uptake efficiency or in predator defence).

We parameterise the model to represent a typical plankton community, where N is associated to nitrogen, P_j correspond to the densities of phytoplankton species and Z to that of a zooplankton predator (see Table 1 in Appendix S1). We assume that the critical resource requirements R_j^* of prey species are uniformly randomly distributed within the range$[R_{min}^*, R_{max}^*]$ if the number of the prey species is > 10; otherwise, to minimise the role of random choice for small prey communities, the R_j^* are distributed equidistantly. To achieve a consecutive colonisation of the system, prey species with randomly chosen R^* are subsequently introduced with small initial density at random time instances during the first 25% of the total simulation time. Every simulation is based on a new set of traits. Further model details are found in Appendix S1.

RESULTS

Figure 1 shows the simulated abundance distributions of the prey guild for different numbers n of prey species that have subsequently been introduced into the system. A first insight on the relative abundances is provided by the equilibrium rank-abundance curves (McGill *et al.* 2007), constructed for the cases of perfect ($\sigma = 0$) and imperfect ($\sigma = 0.1$) prey selectivity (Fig. 1a and b). The rank-abundance distributions reveal the typical community patterns of a small number of dominant prey species coexisting with a large number of rare species (see Fig. S3 in the online Appendix S4 for an example of empirical data). In particular, the width of the rank-abundance curve indicates the realised prey species richness. Since some of the n introduced prey species cannot survive the invasion process (i.e. their abundance decreases exponentially to extremely low values) this realised species richness is less than n. Nevertheless, for both selectivity scenarios the realised species richness increases with n and can reach high values. In contrast, in the absence of prey selectivity (i.e. proportion-based feeding response, $\sigma \gg 1$) we find that the maximal possible number of coexisting prey species is limited to two (cf. Leibold 1996). Thus, the coexistence of a large number of prey species can be mediated by prey selectivity of the generalist predator.

A drastic difference between perfect and imperfect prey selectivity becomes apparent from the trait-abundance curves, which show the correlation between species abundances and their life trait, R^* (Fig. 1, bottom). For the case of perfect prey selectivity ($\sigma = 0$), with increasing number n of introduced species the trait-abundance distribution is shifted to the left and ultimately only species with low R^* values survive (Fig 1c). Thus, although the total number of coexisting spe-

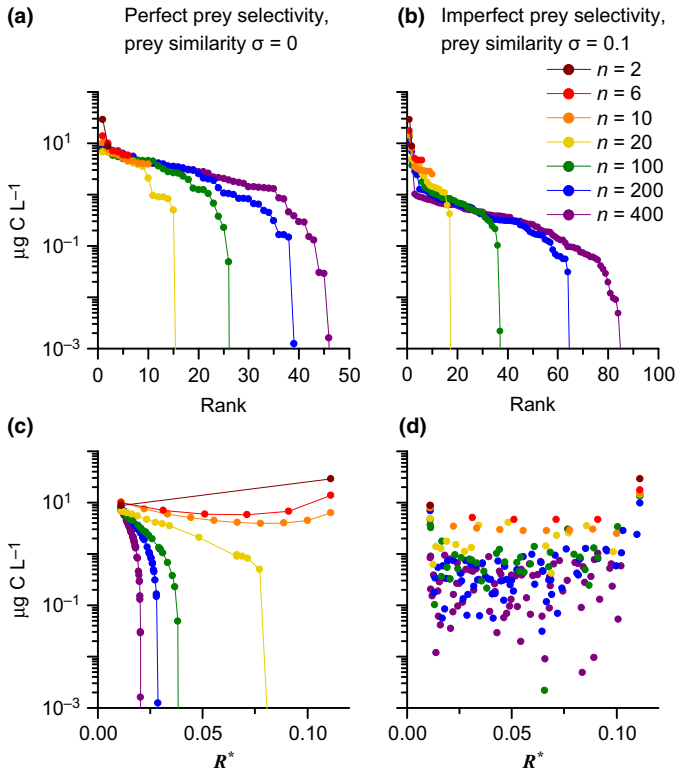

Figure 1 Long-term density distributions of primary producers (P_i) in the food web model. The figure shows the equilibrium density of each species sorted by species rank (i.e. the rank-abundance curve, top panel) and as a function of its R^* value (i.e. the trait-abundance curve, bottom panel). Only the species with a final biomass > 10^{-5} of the most abundant species are shown. Left column: perfect prey selectivity ($\sigma = 0$), right column: imperfect prey selectivity ($\sigma = 0.1$). Different colours indicate the number n of species that have subsequently been introduced into the system (i.e. the number of invasion attempts). Parameter values are provided in Appendix S1.

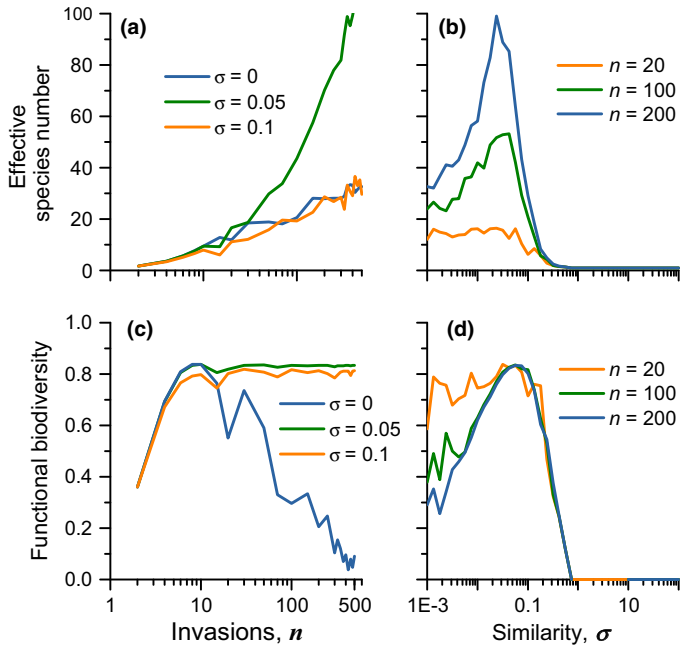

Figure 2 Realised biodiversity of the prey guild. The figure shows the effective species richness (top panel) and the functional biodiversity by Rao's entropy (bottom panel) as functions of the number of introduced species n (left column) and the degree of prey selectivity σ by the predator (right column). Model parameters are as in Fig. 1.

cies formally increases, the functional biodiversity of this assemblage collapses: all surviving species are functionally close to each other and in fact form a single functional group. In contrast, in the case of imperfect prey selectivity ($\sigma = 0.1$) increasing n does not affect the trait range of predator-mediated coexisting competitors, and therefore it does not reduce the functional biodiversity (Fig. 1d). Furthermore, in this case the distribution of species abundances appears to be irregular, which means that the relative abundance of a prey species is weakly correlated with its R^* value. We observe this irregular pattern even after very long simulation times under stationary conditions. In contrast, in the case of perfect prey selectivity, the trait-abundance distribution is highly regular and the relative prey species abundance sharply drops for higher R^* values if the community is large enough (Fig. 1c).

Another difference between the cases of perfect and imperfect prey selectivity is related to the system relaxation time, i.e. the typical time scale for species to reach equilibrium densities. Species densities approach equilibria much faster for perfect selectivity than for imperfect selectivity. In fact, the relaxation times in these two cases differ by more than 1–2 orders of magnitude. In our model the community with $\sigma = 0$ requires ~ 0.5–3 years to reach an equilibrium, whereas for $\sigma = 0.1$ it can take more than 10–100 years. Furthermore, for imperfect selectivity the relaxation time essentially increases with the number of competitors, and the characteristic time scale for species extinction increases with the realised biodiversity (see Appendix S2 for further details).

To quantify the diversity and functionality of the prey community (Mouchet *et al.* 2010) we calculate the effective number of species as the exponential of the Shannon–Wiener index, and the functional biodiversity as Rao's entropy (see Appendix S3 for details). Both for perfect ($\sigma = 0$) and imperfect ($\sigma > 0$) prey selectivity the effective number of coexisting competitors increases with the number n of introduced prey species (Fig. 2a). This increase in realised species richness shows no signs of saturation with further introductions and it is most pronounced for intermediate levels of prey selectivity ($\sigma = 0.05$). In contrast, the indices of functional biodiversity (Fig. 2c) increase with n only for small communities until all open ecological niches are occupied. When this threshold is reached (at about $n \approx 10$ with further species introductions the reaction of the functional biodiversity depends on the degree of prey selectivity: For perfect selectivity ($\sigma = 0$) the functional biodiversity starts to drop with n, whereas for imperfect selectivity ($\sigma > 0$) it reaches a maximum level and becomes independent of n. This difference in the functional diversity for $\sigma = 0$ and $\sigma > 0$ formally reflects the structure of the trait-abundance curves shown in Fig. 1c and d. For perfect prey selectivity the addition of new species leads to a collapse of functional diversity. In contrast, the assumption of imperfect prey selectivity leads to a rather intuitive result:

adding new species, which are similar to the resident species does not affect ecosystem functioning.

The resulting community biodiversity strongly depends on the degree of imperfectness in prey selectivity, σ. For instance, the shift from σ = 0.1 to σ = 0.05 can triple the effective species richness (Fig. 2a). In Fig. 2b and d we show the effective species number and functional biodiversity as functions of σ. In both cases we find a hump-shaped relationship, with a maximal diversity at an intermediate level of prey selectivity (σ ≈ 0.1). For a further increase of σ both diversity indexes decline rapidly, which corresponds to the small prey diversity in the limit of a proportion-based feeding response. Finally, as described above, the effective species number increases with n in the whole range of σ (see Fig. 2b), but the functional diversity gradually decreases with n at small σ (the range of high prey selectivity) and is independent of n for large σ (Fig. 2d).

To assess the role of imperfectness in prey selectivity for diversity-productivity relationships, we explore the effect of eutrophication (an increase of N_0) on the effective species number and functional biodiversity of the prey guild. For the scenario of imperfect prey selectivity (σ = 0.1), both biodiversity characteristics exhibit a hump-shaped dependence on the resource supply (solid curves in Fig. 3). In accordance with the theory of apparent resource competition (Leibold 1996) we obtain the dominance of good nutrient competitors at low concentrations of the supplied resource, the dominance of better defended prey with high resource requirements at high N_0 (i.e. the dominance of prey with large resource requirements and low attack rates from predators due to the built-in trade-off), and the maximal biodiversity at intermediate N_0 when both the resource and predator limitations play a role (see Appendix S4 for corresponding trait-abundance curves). This hump-shaped relationship is lost with perfect prey selectivity (σ = 0), where both biodiversity measures increase monotonically with N_0 (dashed curves in Fig. 3). Thereby, similar to Fig. 2, the functional diversity is greatly reduced with the introduction of new prey species for (σ = 0), but it is retained for imperfect prey selectivity.

To study the influence of the prey community diversity more systematically, in Fig. 4 we investigate the ambient resource concentrations and the total biomass accumulated in each trophic level in dependence of the number of introduced prey species n. Assuming perfect prey selectivity (σ = 0) we find that an increase in n leads to a drastic decrease in predator density, whereas the overall prey density increases (blue curves, see also Prowe *et al.* 2012b) – which leads us to the counterintuitive conclusion that an abundant and diverse prey community might favour predator extinction (Fig. 4a). This peculiar behaviour does not occur in the more realistic scenario of imperfect food selectivity. In this case (σ > 0), the realised biomasses vary with the number of introduced prey only for small community sizes, when all prey species are well distinguishable and the predator must choose between these prey types. As soon as all functional niches are occupied (for the given parameters at about $n \approx 10$, further species introductions do not change the overall prey and predator biomass, or the resource concentration. In particular, in this case a large prey community does not drive the predator towards extinction.

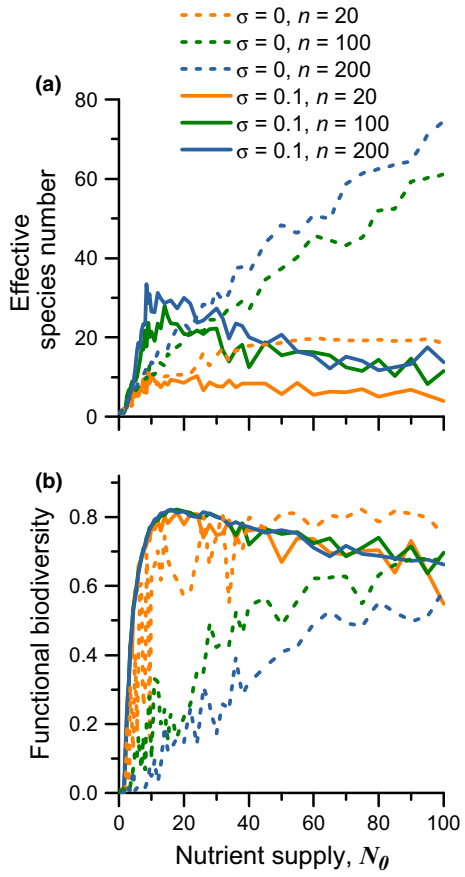

Figure 3 Effect of nutrient enrichment on biodiversity. (a) Effective species number and (B) functional biodiversity by Rao's entropy in dependence of the nutrient supply N_0, for the case of perfect prey selectivity (σ = 0, dashed curves) and imperfect prey selectivity (σ = 0.1., solid curves). Different colours indicate the number of introduced species n = 20 (orange), n = 100 (green) and n = 200 (blue). Model parameters are as in Fig. 1.

The mechanism for the discrepancy between the scenarios of perfect and imperfect prey selectivity can be related to the structure of the intake rate (1). Perfect selectivity assumes that the preference for each prey species is proportional to its relative abundance, see (2). However, the accumulated biomass per species decreases with the number of species in the system, so, in the case of perfect selectivity the intake rate vanishes for diverse prey communities (see eqn (3) and Appendix S6). As a consequence, with increasing prey diversity, the system undergoes a transition from a predator driven community to a community shaped by competition for the limiting resource, in which prey species with the lowest resource requirements dominate (see Fig 1c). In contrast, the scenario of imperfect switching assumes that the preference ρ_i for a particular prey species i depends on the total abundance of the whole functional group, which in turn is only weakly related to the overall biodiversity, provided that all ecological niches are occupied. Thus, in the case of imperfect prey selectivity, the intake rate does not vanish with increasing prey biodiversity, and the same mechanism mediating the coexistence of a few prey species is retained for dozens of species.

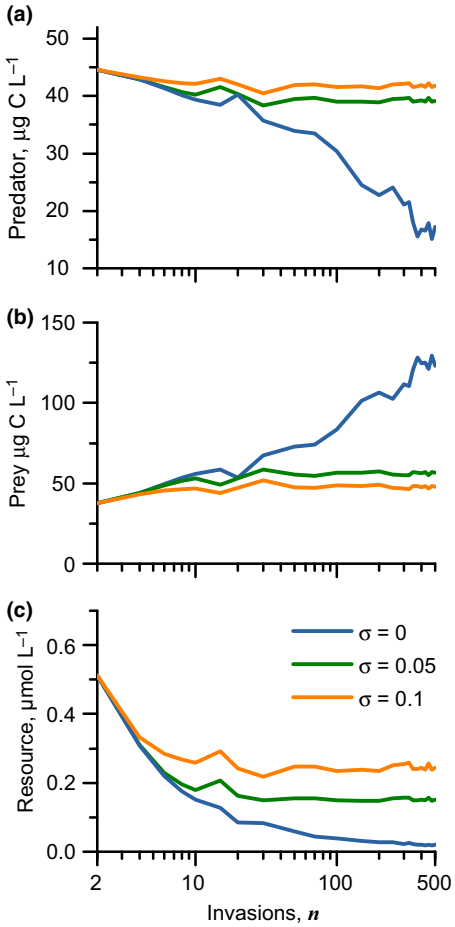

Figure 4 Effect of the number of introduced species n on the total predator biomass Z (top panel), the total biomass of primary producers $\sum P_i$ (middle panel), and the resource concentration N, for different levels of prey selectivity, $\sigma = 0$ (blue), $\sigma = 0.5$ (green) and $\sigma = 0.1$ (orange). Model parameters are as in Fig. 1.

DISCUSSION

We have introduced a functional response with imperfect prey selectivity by a generalist predator feeding on multiple prey. The main novelty here is that the preference for a certain prey species depends not only on the relative abundance of this prey but also on the abundances of other functionally close species. Thus, our approach combines patterns of selectivity for distinctly different prey species with patterns of proportion-based consumption within a group of prey with close life traits. Implementation of the new functional response in a generic food web model reveals important consequences for ecosystems functioning. It provides a straightforward solution to the famous paradox of plankton – the possibility of coexistence of a large number of species in an apparently homogeneous environment – and at the same time it is free from several biological artefacts inherent to the perfect switching scenario.

Our model can explain the high biodiversity observed in communities of species competing over a limited number of resources. The maximal effective species richness and functional diversity is reached for an intermediate level of prey selectivity. In this range of imperfect prey selectivity our model is able to reproduce the characteristic shape that is observed in empirical abundance distributions (see online Appendix S4). Compare, for example our simulated rank-abundance curves (Fig. 1b and Fig. S2) with Fig. S3, which shows a typical rank-abundance distribution of a phytoplankton community in Lake Lugano (Pomati *et al.* 2011). In contrast, we were not able to match empirical abundance distributions with perfect prey selectivity: the simulated rank-abundance curves are always either flat or concave and do not show a group of highly abundant species (Fig. 1a, Fig. S2).

Our study provides a new solution to the long-standing ecological enigma of why plankton communities are never at equilibrium (Scheffer *et al.* 2003). We show that the assumption of imperfect predator switching results in extremely long times required to achieve equilibrium: non-equilibrium patterns are found even after more than 100 years of simulation time under stationary environmental conditions. The enlarged relaxation times can be explained by our key assumption that grazing depends on the total abundance of functionally close prey. Thus, density fluctuations within a functional prey group can compensate each other as they are added up in the grazing rate. Thereby, the feedback between abundance fluctuations and species specific grazing pressure is suppressed and all fluctuations decay extremely slowly, which can strongly limit our ability to observe ecological equilibria in realistic conditions.

We have shown that the assumption of perfect selectivity, which has been widely used to explain prey biodiversity, leads to a number of artefacts. In particular, increasing prey diversity n leads to a collapse of prey functional biodiversity (Fig. 1c) and to a decrease in the predator biomass with a simultaneous increase in the total prey biomass (Fig. 4). We have demonstrated that these effects mechanistically originate in a severe dilution effect, i.e. the reduction in feeding rates with increasing number of prey species (2). In contrast, these artefacts disappear with imperfect selectivity. In this case, increasing prey diversity n increases or has no effect on the functional biodiversity (Fig. 1c). The decay of predator biomass with increasing prey biomass arises only for small n where some ecological niches are available (Fig. 4). As soon as all ecological niches are occupied, any further increase in n does not affect the total prey and predator biomass. These findings are in agreement with experimental results (Loreau & Hector 2001) which show a saturation of productivity with increasing consumer richness.

Our results are in good agreement with keystone predation competition theory (Leibold 1996). Assuming a trade-off between prey resource requirements and vulnerability to predation, we find that with increasing nutrient loads the dominance of good nutrient competitors is replaced with the dominance of predator resistant prey species (Fig. S2). The transition in the prey assemblage can result in a hump-shaped diversity-productivity relationship, with a maximal biodiversity at an intermediate nutrient load (Fig. 3) – in accord to empirical observations (Chase & Leibold 2003).

We intentionally kept the model simple to identify the main mechanism of species coexistence. In particular, we varied only

two traits of the prey species: half-saturation constants vs. attack rates, we restricted the analysis to equilibrium situations and we did not consider the case of multiple predator species. While our findings are fairly robust, we found that the way we link the pairwise prey similarities ε_{ij} with species traits may play an important role. To test this we first assigned prey similarities in a random way, resulting in less diverse prey communities as the consumption of similar prey species with essentially different traits becomes density proportional and the outcome follows the keystone predation model. Second, we examined another generic case, when the prey similarities ε_{ij} in eqn (5) decay as a Gaussian function (see Appendix S5). Our main findings were unaffected, however, the competing species appear to form clusters of functionally similar prey species in niche space. Namely, the distribution of species over the trait axis is not homogenous as in Fig. 1d, but instead approaches a function with strong peaks at singular values of R^*, separated by almost empty ranges in which all competitors become extinct. Such clustering can provide a possible explanation for the non-homogeneous distribution of species in life traits that has been observed in empirical studies (e.g. Havlicek & Carpenter 2001; Litchman *et al.* 2009). The emergence of species clustering was previously found in other models using a non-local competition kernel (Roughgarden 1998; Scheffer & van Nes 2006). Our work emphasises a strong sensitivity of this phenomenon on the particular choice of this function (cf. Pigolotti *et al.* 2007). Notwithstanding, the other our conclusions are largely independent from the specific analytic form, and the associated ecological assumptions, of the used functional response. We have obtained qualitatively the same results with the functional response by Morozov & Petrovskii (2013) and with different parameterisations of our functional response (Appendix S7).

Overall, revealing the 'true' multi-prey functional response of a generalist predator remains a challenge. Even though active predator switching is well documented in natural ecosystems (Murdoch 1969; Gentleman *et al.* 2003), empirical support for imperfect switching is hard to come by. There is ample evidence that switching is related to a learning effect, search image formation or behavioural changes in foraging mode that increase the rate of encounter of certain prey species at the expense of encounters with others (Allen 1988; Loeuille 2010). Thereby predators frequently select for prey that are different in more or less continuous life traits, such as body size, colour, mobility, or habitat choice (Hughes & Croy 1993; Elliott 2006; Bond 2007; Saha *et al.* 2010; Klecka & Boukal 2012) – corresponding to our formulation of prey similarity in trait space, Eq (5). In this generic situation imperfect selection will result from any proximate mechanism that will cause a predator to select prey only within a degree of uncertainty in trait space, as expressed by our imperfectness parameter σ. For instance, many predators cannot easily distinguish close colours or shapes (Allen 1988; Bond 2007) or focus on prey from a narrow size range (Elliott 2006; Saha *et al.* 2010) so that the discovery or intake rate will be disproportionally higher for prey with close traits to the preferred prey, even if they are rare. As shown in our model simulations this effect has drastic consequences on a community level already when the level of imperfectness σ is very small. Thus, our model results should be relevant for a wide range of ecological situations where predators can select for prey from a continuous spectrum of life traits.

Our theoretical results suggest that we may need to rethink the role of generalist predators in maintaining diversity. Further progress will ultimately depend on testing our predictions in natural communities. One crucial step in this direction will be the direct evaluation of the multi-species functional response in empirical studies or in laboratory experiments, which would require the precise measurement of predation rates for different combinations of prey frequencies. Ideally such experiments would be designed to allow a control of trait similarity (e.g. by different prey selections from a continuous spectrum of life traits, as described above) or imperfectness of prey selectivity (e.g. by manipulating the predator's search image formation or prey detection ability). In the least, such experiments should involve three prey species, but more informative results could be achieved with larger prey communities of more than 10 species, which would allow to observe rank-abundances curves, biomass distributions across life-history traits of prey and variability among prey. The combination of such empirical investigations with theoretical studies could provide us with the crucial information needed to advance our understanding about the role of imperfect prey selectivity for promoting biodiversity and irregularity in food webs.

ACKNOWLEDGEMENTS

A.B.R. acknowledges support from the Helmholtz Virtual Institute (VH-VI-500, PolarTime).

AUTHORSHIP

All authors designed this study. ABR and AM performed numerical simulations. All authors contributed substantially into writing the manuscript.

REFERENCES

Abrams, P.A. & Matsuda, H. (2003). Population dynamical consequences of reduced predator switching at low total prey densities. *Popul. Ecol.*, 45, 175–185.

Allen, J.A. (1988). Frequency-dependent selection by predators. *Philos. Trans. R. Soc. London B*, 319, 485–503.

Amarasekare, P. (2003). Competitive coexistence in spatially structured environments: a synthesis. *Ecol. Lett.*, 6, 1109–1122.

Bond, A.B. (2007). The evolution of color polymorphism: crypticity, searching images, and apostatic selection. *Annu. Rev. Ecol. Evol. Syst.*, 38, 489–514.

Chase, J.M. & Leibold, M.A. (2003). *Ecological Niches: Linking Classical and Contemporary Approaches*. University of Chicago Press, Chicago, IL.

Edwards, K.F., Klausmeier, C.A. & Litchman, E. (2011). Evidence for a three-way trade-off between nitrogen and phosphorus competitive abilities and cell size in phytoplankton. *Ecology*, 92, 2085–2095.

Elliott, J.M. (2006). Prey switching in *rhyacophila dorsalis* (trichoptera) alters with larval instar. *Freshw. Biol.*, 51, 913–924.

Follows, M.J., Dutkiewicz, S., Grant, S. & Chisholm, S.W. (2007). Emergent biogeography of microbial communities in a model ocean. *Science*, 315, 1843–1846.

Gentleman, W., Leising, A., Frost, B., Storm, S. & Murray, J. (2003). Functional responses for zooplankton feeding on multiple resources: a

review of assumptions and biological dynamics. *Deep-Sea Res. II*, 50, 2847–2875.

Greenwood and Elton (1979). Analysing experiments on frequency-dependent selection by predators. *J. Anim. Ecol.*, 48, 721–737.

Hambäck, P.A. (1998). Seasonality, optimal foraging, and prey coexistence. *Am. Nat.*, 152, 881–895.

Havlicek, T. & Carpenter, S.R. (2001). Pelagic species size distributions in lakes: are they discontinuous? *Limnol. Oceanogr.*, 46, 1021–1033.

Holt, R.D., Grover, J.P. & Tilman, D. (1994). Simple rules for interspecific dominance in systems with exploitative and apparent competition. *Am. Nat.*, 144, 741–771.

Hughes, R.N. & Croy, M.I. (1993). An experimental analysis of frequency-dependent predation (switching) in the 15-spined stickleback, Spinachia spinachia. *J. Anim. Ecol.*, 62, 341–352.

Huisman, J., Johansson, A.M., Folmer, E.O. & Weissing, F.J. (2001). Towards a solution of the plankton paradox: the importance of physiology and life history. *Ecol. Lett.*, 4, 408–411.

Hutchinson, G.E. (1961). The paradox of the plankton. *Am. Nat.*, 95, 137–145.

Hutson, V. (1984). Predator mediated coexistence with a switching predator. *Math. Biosci.*, 68, 233–246.

Ives, A.R. & Carpenter, S.R. (2007). Stability and diversity of ecosystems. *Science*, 317, 58.

Kiørboe, T., Saiz, E. & Viitasalo, M. (1996). Prey switching behaviour in the planktonic copepod Acartia tonsa. *Mar. Ecol. Prog. Ser.*, 143, 65–75.

Klecka, J., Boukal, D.S. (2012). Who Eats Whom in a Pool? A Comparative Study of Prey Selectivity by Predatory Aquatic Insects. PLoS ONE, 7 (6): e37741. doi:10.1371/journal.pone.0037741

Koen-Alonso, M. & Yodzis, P. (2005). Multispecies modeling of some components of the marine community of northern and central Patagonia. *Argentina. Can. J. Fish. Aqu. Sciences*, 62, 1490–1512.

Kondoh, M. (2003). Foraging adaptation and the relationship between food-web complexity and stability. *Science*, 299, 1388–1391.

van Leeuwen, E., Brännström, Å., Jansen, V.A.A., Dieckmann, U. & Rossberg, A.G. (2013). A generalized functional response for predators that switch between multiple prey species. *J. Theor. Biol.*, 328, 89–98.

Leibold, M.A. (1996). A graphical model of keystone predators in food webs: trophic regulation of abundance, incidence, and diversity patterns in communities. *Am. Nat.*, 147, 784–812.

Litchman, E., Klausmeier, C.A. & Yoshiyama, K. (2009). Contrasting size evolution in marine and freshwater diatoms. Proceedings of the National Academy of Sciences, 106, 2665–2670.

Loeuille, N. (2010). Consequences of adaptive foraging in diverse communities. *Funct. Ecol.*, 24, 18–27.

Loreau, M. & Hector, A. (2001). Partitioning selection and complementarity in biodiversity experiments. *Nature*, 412, 72–76. doi: 10.1038/35083573.

McGill, B.J., Etienne, R.S., Gray, J.S., Alonso, D., Anderson, M.J., Benecha, H.K., *et al.* (2007). Species abundance distributions: moving beyond single prediction theories to integration within an ecological framework. *Ecol. Lett.*, 10, 995–1015.

Monod, J. (1950). La technique de la culture continue: Theorie et applications. Ann. Inst. Pasteur 79, 390–410.

Morozov, A.Y. & Petrovskii, S.V. (2013). Feeding on multiple sources: towards a universal parameterization of the functional response of a generalist predator allowing for switching. *PLoS ONE*, 8, e74586. doi: 10.1371/journal.pone.0074586.

Mouchet, M.A., Villéger, S., Mason, N.W.H. & Mouillot, D. (2010). Functional diversity measures: an overview of their redundancy and their ability to discriminate community assembly rules. *Funct. Ecol.*, 24, 867–876.

Murdoch, W.M. (1969). Switching in general predators: experiments on predator specificity and stability of prey populations. *Ecol. Monogr.*, 39, 335–354.

Pigolotti, S., López, C. & Hernández-García, E. (2007). Species clustering in competitive Lotka-Volterra Models. *PRL*, 98, 258101.

Pomati, F., Jokela, J., Simona, M., Veronesi, M. & Ibelings, B.W. (2011). An automated platform for phytoplankton ecology and aquatic ecosystem monitoring. *Environ. Sci. Technol.*, 45, 9658–9665.

Proulx, M.F.R., Pick, A., Mazumder, P.B., Hamilton, P.B. & Lean, D.R.S. (1996). Experimental evidence for interactive impacts of human activities on lake algal species richness. *Oikos*, 76, 191–195.

Prowe, A.E.F., Pahlow, M., Dutkiewicz, S., Follows, M. & Oschlies, A. (2012a). Top-down control of marine phytoplankton diversity in a global ecosystem model. *Prog. Oceanogr.*, 101, 1–13.

Prowe, A.E.F., Pahlow, M. & Oschlies, A. (2012b). Controls on the diversity productivity relationship in a marine ecosystem model. *Ecol. Model.*, 225, 167–176.

Risch, S.J. & Carroll, C.R. (1982). Effect of a keystone predaceous ant, Solenopsis geminata, on arthropods in a tropical agroecosystem. *Ecology*, 63, 1979–1983.

Roughgarden, J. (1998). *Primer of Ecological Theory*. Prentice Hall, Upper Saddle River, New Jersey.

Roughgarden, J. & Feldman, M. (1975). Species packing and predation pressure. *Ecology*, 56, 489–492.

Roy, S. & Chattopadhyay, J. (2007). Towards a resolution of '*the paradox of the plankton*': a brief overview of the proposed mechanisms. *Ecol. Complex.*, 4, 26–33.

Ryabov, A.B. & Blasius, B. (2011). A graphical theory of competition on spatial resource gradients. *Ecol. Lett.*, 14, 220–228.

Saha, N., Aditya, G., Saha, G.K. & Hampton, S.E. (2010). Opportunistic foraging by heteropteran mosquito predators. *Aquat. Ecol.*, 44, 167–176.

Scheffer, M. & van Nes, E.H. (2006). Self-organized similarity, the evolutionary emergence of groups of similar species. *PNAS*, 103, 6230–6235.

Scheffer, M., Rinaldi, S., Huisman, J. & Weissing, F.J. (2003). Why plankton communities have no equilibrium: solutions to the paradox. *Hydrobiologia*, 491, 9–18.

Smout, S., Asseburg, C., Matthiopoulos, J., Fernández, C., Redpath, S., Thirgood, S. & Harwood, J. (2010). The functional response of a generalist predator. *PLoS One.*, 5: e10761.

Strom, S.L. & Loukos, H. (1998). Selective feeding by protozoa: model and experimental behaviors and their consequences for population stability. *J. Plankton Res.*, 20, 831–846.

Tilman, D. (1982). *Resource Competition and Community Structure*. Princeton University, Princeton.

SUPPORTING INFORMATION

Additional Supporting Information may be downloaded via the online version of this article at Wiley Online Library (www.ecologyletters.com).

Editor, Gregor Fussmann
Manuscript received 29 June 2015
First decision made 30 July 2015
Manuscript accepted 16 August 2015

Supporting information

Imperfect prey selectivity of predators promotes biodiversity and irregularity in food webs

Alexey B. Ryabov, Andrew Morozov, Bernd Blasius

Appendix 1. Model parameters and simulation details.

Numerical simulations of food web model (see equations (6)-(8) in the main text) were conducted for parameters describing the dynamics of a typical plankton community. See Table 1 for the parameter values and possible ranges.

In simulations of the model with a large number of prey species (*n*>10) the values of H_i were randomly drawn from a uniform distribution within the interval [0.1, 1]. Otherwise, in simulations with a smaller number of phytoplankton species (*n* <10), the H_i were equidistantly distributed within this interval to avoid the undesirable situation of grouping the H_i by random initial choice. Our model results are generally preserved if we distribute the H_i equidistantly in all simulations (also for *n*>10), however the number of surviving species then increases. We assumed a linear trade-off between the predator attack rate on species i, a_i, and the resource requirement of this species, characterized by its half-saturation constants H_i (see (10) main text)

$$a_i = a_{max} - (H_i - H_{min})\frac{a_{max}-a_{min}}{H_{max}-H_{min}},$$

with $a_{max} = 0.1$, $a_{min} = 0.01$, $H_{max} = 1.0$, $H_{min} = 0.1$. Thus, the vulnerability of phytoplankton species increases with decreasing resource requirements. For the sake of simplicity, we further assumed that the handling time of the predator is constant for all species: h = 1 day.

To find an equilibrium state, we have conducted numerical simulations of the model for 200,000 simulation days for imperfect predator selectivity ($\sigma > 0$) and 20,000 days for perfect predator selectivity ($\sigma = 0$). The difference in the simulation time was caused by the different rates of approach to an equilibrium state: In comparison with perfect prey selectivity, imperfect selectivity leads to much slower relaxation processes (see Appendix 2).

The phytoplankton (prey) species were introduced successively into the system during the first 25% of the whole simulation time at random time instances with an initial density that was randomly drawn from a uniform distribution in the range from 0 to 0.01 µg C/l. For comparison, we have also performed simulations where all species were introduced simultaneously at the start of the simulation, $t = 0$. Both simulations showed similar results; however, the number of surviving species was sometimes 50% greater when the species were introduced subsequently. Thus, the final abundance distribution is sensitive to the history of community assembly (cf. Fukami and Morin 2003).

Modelling the dynamics of more than 100 species for such long simulation times is extremely time demanding, and to simulate results for a given combination of the model parameters we used only one set of randomly chosen species traits. To avoid the bias caused by the trait selection we used independent sets of species traits for different parameter combinations. For instance, every data point on every line in Fig. 2 corresponds to a simulation with independent sets of H_i, a_i, different invasion times and invasion sequences. This results in somewhat irregular patterns in this and similar figures. In spite of this irregularity, the general pattern is clearly visible, and we are

confident that adding more simulations will not change the general results.

The obtained set of equations was solved using the MATLAB 2011 routine ode45 with relative and absolute accuracy equal to 10^{-10}. During the simulation time, we tracked the abundances of all species independent of their biomass. Thus, any species could reinvade the system if, for instance, this species could not survive in the initial community, but could survive after invasion of other competitors. To plot rank-abundance and trait-abundance curves we used only the species with a final biomass that was greater than 10^{-5} of the most abundant species biomass.

Table1 Model parameters

Parameter	Value	Units	Meaning	Reference
Nutrient				
D	0.1	day^{-1}	Nutrient supply (exchange) rate	[3]
N_0	25 (1…100)	μ mol N/l	Equilibrium nutrient concentration	[3]
Phytoplankton				
H	0.1…1	μ mol N/l,	Half-saturation constant for nutrient	[3]
μ	1	day^{-1}	Maximal growth rate	[11]
α	1/7	μ mol N/ μ mol C	Amount of nitrogen consumed to produce 1 μ mol C	[10]
m	0.1	day^{-1}	Background mortality	[6,7]
Zooplankton				
θ	0.25		Assimilation efficiency	[7]
m_Z	0.075	day^{-1}	Zooplankton mortality	[6]
a_i	0.1…0.01	(μmol C day)$^{-1}$	Zooplankton attack rate	[3, 6, 7]
η_i	1		Density-independent preference	
h	1	day	Zooplankton handling time	[6]

Appendix 2. Computation of the relaxation time of the system

The relaxation time characterizes the time scale at which a system approaches an equilibrium state. To find the relaxation time we assumed that the absolute difference between the species density N_i and the final density N_i^{fin} ultimately decays exponentially

$$|N_i(t) - N_i^{fin}| \sim Be^{-t/\tau} ,$$

where τ is the characteristic relaxation time. We determined τ as the best-fit parameter in the range where the deviation from the final density decreases from 10^{-4} to 10^{-7} μg C/l (see Fig. S1A). The relaxation time was measured for each competitor separately (Fig. S1B and C). The overall relaxation time of the system was estimated as the average relaxation time of all competitors.

Assuming imperfect prey selectivity of the predator, we find that the relaxation time becomes several orders of magnitude larger compared to the scenario with perfect prey selectivity (Fig. S1B and C). This finding is robust within a wide range of species parameters. Furthermore, the relaxation time, and therefore also the extinction time, increases largely with the number of prey species n (see different colors in Fig S1 B and C). For instance, modelling the dynamics of 1000 prey species we were unable to approach an ecological equilibrium even after 500 years of simulation time.

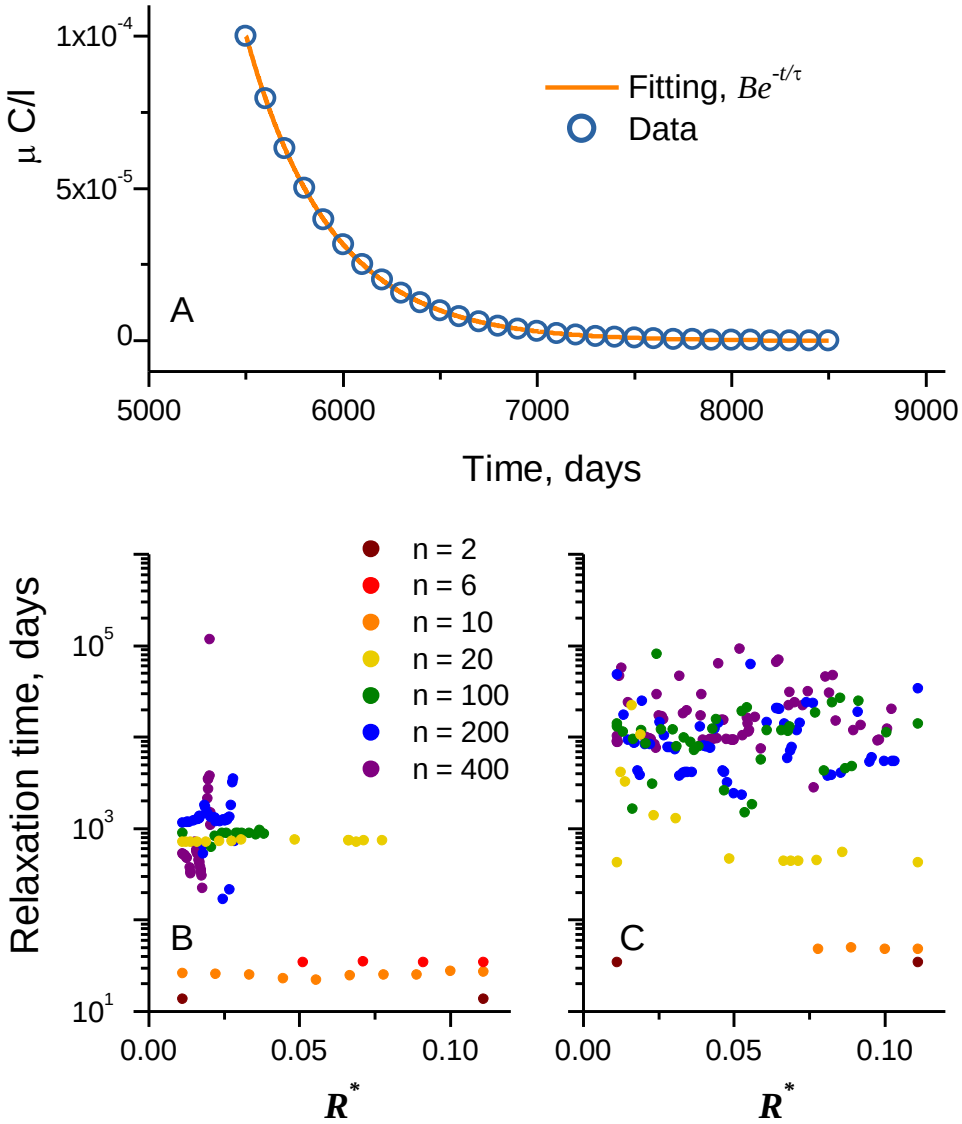

Fig. S1. Simulated relaxation time to equilibrium. (A) Computation of the relaxation time. Blue dots show a typical time course of the difference between the density of species at time t and its equilibrium value. The orange line shows the best-fit of the function $Be^{-t/\tau}$ to the simulated data points. (B, C) The relaxation time of prey species as a function of R^*, in the case when the predator selectivity is perfect, $\sigma = 0$ (B) and imperfect, $\sigma = 0.1$ (C). Different colors represent different numbers of introduced prey species in the system.

3. Defining biodiversity indexes

To assess the effective number of species we use the classical Shannon–Wiener entropy

$$H = -\sum_i p_i \ln p_i \,,$$

where p_i is the relative abundance of species i. The effective number of species in the system is given by

$$n_{eff} = exp(H).$$

If the abundances of all competitors are equal, n_{eff} gives the overall number of species (species richness). The effective number of species approaches one when only one competitor dominates the system, while the other species are extremely rare. In general, n_{eff} reflects the number of mostly common species, and therefore it decreases with the evenness of the species abundance distribution.

To assess the evenness we applied Pielou's index (Pielou 1966)

$$J = \frac{H}{H_{max}},$$

where H is the Shannon–Wiener entropy and $H_{max} = \ln n$ is the maximal Shannon entropy of n species.

The functional biodiversity can be estimated in a variety of ways (Mouchet et al. 2010). Here, we calculate the functional biodiversity based on Rao's entropy (Botta-Dukát 2005)

$$Q = \sum_{i=1}^{n-1} \sum_{j=i+1}^{n} d_{ij} p_i p_j,$$

where d_{ij} is the dissimilarity between the species i and species j ($d_{ij} = d_{ji}$ and $d_{ii} = 0$).

We calculated the interspecific dissimilarity based on the critical resource requirement R_j^* as

$$d_{ij} = 1 - exp\left(-\frac{\left(R_i^* - R_j^*\right)^2}{\Delta R^2}\right).$$

We used this form to obtain the best visual representation of the functional biodiversity as a function of species number (see Fig. 2C in the main text). Here $\Delta R = 0.01$ µmol N/l defines the characteristic distance between species within the same functional group. If the difference $R_i^* - R_j^*$ is less than ΔR, i.e. the competitors are similar and belong to the same functional group, then d_{ij} approaches zero. By contrast, if the difference between the critical resource values of the competitors is sufficiently large, then d_{ij} approaches one. Thus, the species dissimilarity represents an inverse quantity to the species similarity, if we define the similarity by the Gaussian function (see Appendix 5).

Note that one can use other definitions for the interspecific dissimilarity, for instance, based on the Euclidian distance (Botta-Dukát 2005)

$$d_{ij} = \left(R_i^* - R_j^*\right)^2.$$

This mainly affects the results for the model with perfect prey selectivity. In particular, the decay of the blue curve in Fig.2C (see the main text) will be steeper, while the green and orange curves will remain the same.

Appendix 4. Rank-abundance curves across different levels of eutrophication

An increase of the nutrient supply concentration affects the community structure differently in the model with perfect and imperfect prey selectivity of the predator (Fig. S2). Assuming perfect prey selectivity, an increase of N_0 leads to an increase of species richness (Fig. S2A), however, it does not change the community structure as good nutrient competitors always dominate (Fig. S2D). Our simulation shows that Pielou's evenness increases abruptly with N_0 and levels off at about $N_0 = 10$ (Fig. S2C, blue line).

By contrast, if predator food selectivity is imperfect, an increase of nutrient loads does not have a similar strong effect on prey richness; it rather affects the community structure. Only for small N_0 the species richness increases with nutrient concentrations, as prey with high resource requirements obtain new niches (Fig. S2B). A further increase of N_0 does not affect species richness, but decreases the effective species number (Fig. 4A, main text) because the evenness of species distribution starts to decrease (Fig. S2C, orange line). The hump-shaped dependence of species biodiversity and evenness on the resource supply reflects the transition in the species composition shown in Fig. S2E. Namely, at small N_0 prey with low resource requirements dominate (yellow dots), while at high N_0 prey with high R^* values but low attack rates dominate (green and blue dots). Both these configurations lead to low evenness and low biodiversity. By contrast, at intermediate N_0 all prey species can coexist (orange dots), resulting in the maximum of evenness and biodiversity. Thus, we retrieve the results of the keystone predation model (Leibold, 1996).

To characterize the community composition we also calculate the weighted average R^*-value

$$< R^* >= \sum_i p_i R_i^* ,$$

which represents the "average" resource requirement of the community. In the model with perfect prey selectivity, $< R^* >$ reaches only small values (Fig. S2F, blue curve). By contrast, assuming imperfect selectivity we find that $< R^* >$ changes in a much wider range, which reflects the transition from good nutrient competitors to the predator resistant prey (Fig.S2F, orange curve).

Compare now the shape of the rank-abundance curves shown in Fig. S2 A and B with a typical shape obtained from empirical studies. An example of field data by Pomati et al. (2011) on the phytoplankton community in Lake Lugano is shown in Fig. S3. This example demonstrates three characteristic segments of a rank-abundance distribution, exhibited by the following species groups: I) the dominant group of the most abundant species with the smallest rank, II) the group of rare species, whose abundances decay nearly exponentially with the rank, and III) the group of extremely rare species, whose abundances drop with rank faster than exponentially. The last two groups appear in both our models (with or without perfect prey selectivity, see Fig. S2 A and B). However, the group of the most abundant species (segment I) appears only in the model with imperfect prey selectivity (see inset in Fig. S2B), while we could not reproduce this segment in the model with perfect prey selectivity: the rank-abundance curve was always either flat or concave (see inset in Fig. S2A).

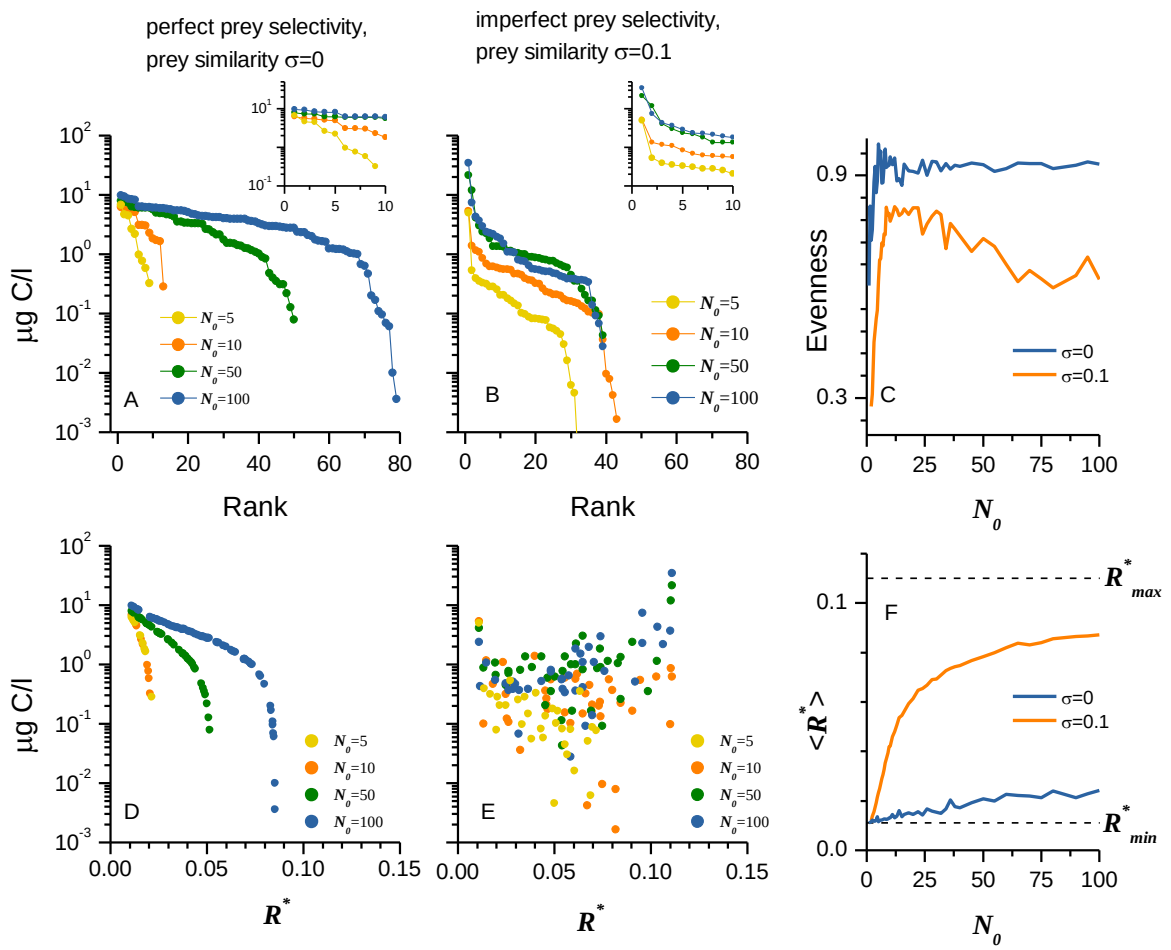

Fig. S2. Effect of the nutrient supply concentration N_0 on the prey community structure. (A,B) rank-abundance curves and (D,E) trait-abundance curves for four different levels of N_0, assuming perfect (left panel) and imperfect (middle panel) predator selectivity. Insets in (A, B) enlarge the community structure for the most dominant species. The right panel shows the evenness and average R^* value of the community as a function of N_0.

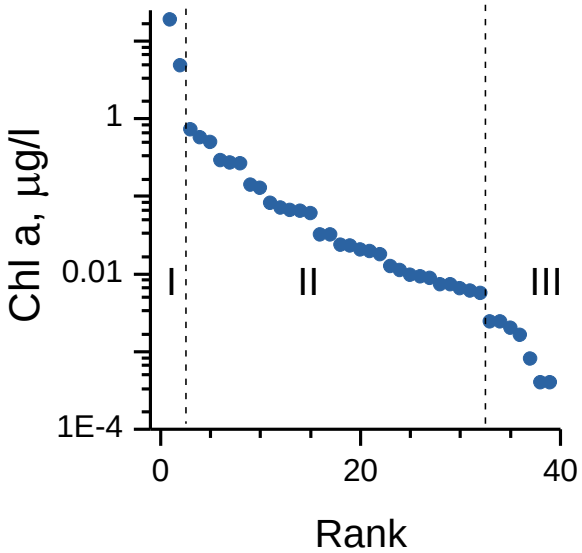

Fig. S3. Exemplary rank abundance distribution of a freshwater phytoplankton community (data points show the 2010 spring bloom in lake Lugano, Pomati et al. 2011). The roman numerals indicate the three characteristic segments of a rank-abundance distribution: I) group of the most abundant species, II) group of rare species with exponentially decay in rank abundance, and III) group of extremely rare species whose densities drop with rank faster than exponentially.

Appendix 5. Emergence of clusters in niche space

In the main text, we assumed that the pairwise similarity of prey species ε_{ij} is an exponentially decaying function of the difference between the species half-saturation constants (Eq (5), main text). Here we briefly address another biologically possible scenario, where the ε_{ij} are described by a Gaussian function

$$\varepsilon_{ij} = \exp\left(-\frac{\left| H_i - H_j \right|^2}{\sigma^2} \right).$$

The implementation of the Gaussian function in the food web model does not affect the main findings of our paper (see Fig. S4). In particular, imperfect prey selectivity of the predator still leads to high biodiversity of the prey community, with a maximum at an intermediate value of σ (compare with Fig. 2B). Only, the absolute level of biodiversity is typically smaller than in the model with exponential similarity decay.

The most striking effect of the change in the functional form is the emergence of clustering (limiting similarity) in the trait-abundance distribution of prey (see Fig. S4). These clusters of prey species can be clearly seen if the trait values (resource requirements of prey species) are equidistantly distributed along the niche axes and all species start to grow simultaneously (Fig. S4B). These clusters form functional groups of prey species, with the distance between the groups depending on the parameter σ. If prey species belong to different groups, then the predator can distinguish between them. Therefore, competition between these species follows the rules of the model with perfect prey selectivity and these species can coexist. By contrast, within every cluster the prey species are quite similar (as the Gaussian function decay only quadratically at the origin). Thus, competition between prey species from the same group closely follows the rules of the model with no selectivity. As a result, only one or two competitors in each group can ultimately survive. However, this selection process is extremely slow as these competitors also possess very close trait values. Therefore, the appearance of the clusters is a long-lasting transient process. For instance a five times increase of the simulation time does not drastically change the cluster structure (compare the results after 20,000 and 100,000 simulation days shown in Fig. S3B as the red and grey dots, respectively).

For a Gaussian similarity decay a clear cluster structure, however, is a fragile phenomenon (but see Pigolotti et al. 2007). In particular it does not appear if we assume that the prey species invade at random time points and their resource requirements are randomly distributed (in fact either of these assumptions alone is enough to destroy the clear species lumping). Nevertheless, we still observe the emergence of limiting similarity of the prey. The comparison of simulation results after 30,000 and 100,000 days shows that if the resource requirements of competitors are close then only one or two species can survive, while competitors with sufficiently large difference in resource requirements can coexist (see Fig. S4A, grey and red dots, respectively). As in the previous case, this transient process is extremely slow.

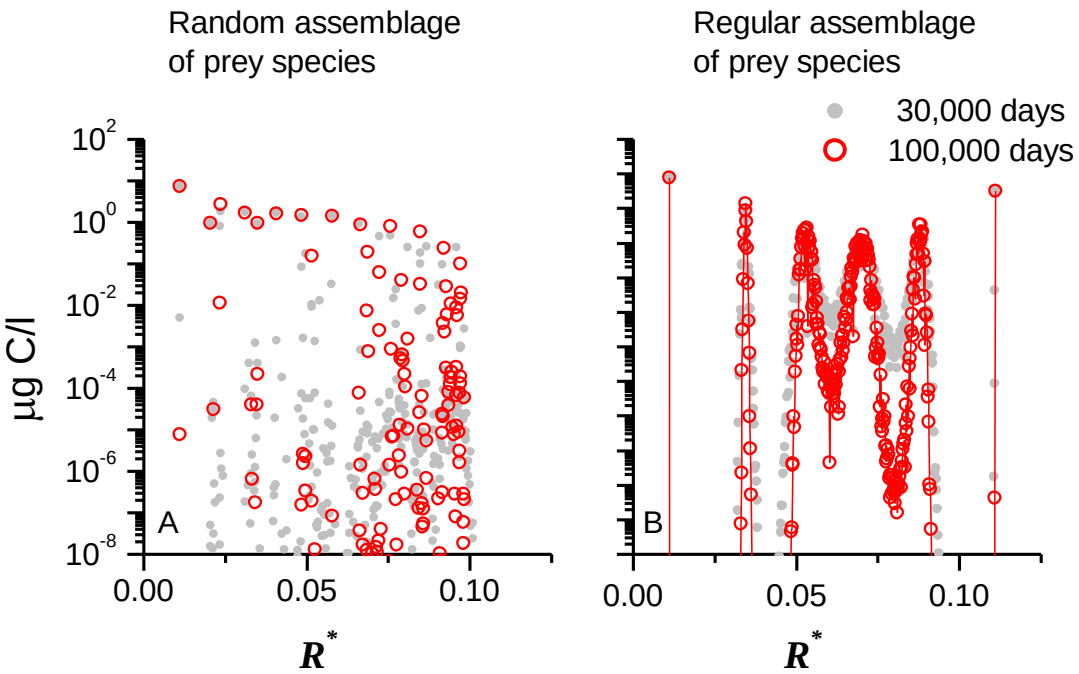

Fig. S4. Gaussian decay of prey similarity leads to clustering of prey species in niche space. The plot shows the long-term distribution of primary producers assuming that ε_{ij} decays as a Gaussian function with the difference in resource requirements after 30,000 days (grey) and 100,000 days (red). (A) Prey species are introduced at random time instances and their resource requirements are uniformly distributed. (B) Prey species are introduced simultaneously at $t = 0$ and their resource requirements are equidistantly distributed. In both cases the initial biomasses of prey species are random. Model parameters are as in Table 1 with the exception of $N_0 = 10$ and $\sigma = 0.05$ (A) and $\sigma = 0.1$ (B).

Appendix 6. Revealing conceptual problems of the multi-prey functional response with a perfect prey selectivity

The multi-prey functional response (1) with perfect selectivity (2) can be expressed as

$$f_i = \frac{a_i \rho_i P_i}{1+\sum_{k=1}^{n} a_k h_k \rho_k P_k} = \frac{a_i \frac{\eta_i P_i}{\sum_{k=1}^{n} \eta_k P_k} P_i}{1+\sum_{k=1}^{n} a_k h_k \frac{\eta_k P_k P_k}{\sum_{k=1}^{n} \eta_k P_k}} = \frac{a_i \eta_i P_i^2}{\sum_{k=1}^{n} \eta_k P_k + \sum_{k=1}^{n} a_k h_k \eta_i P_k^2}$$

The total intake rate of prey by the predator is the sum of prey specific ingestion rates

$$f = \sum_{i=1}^{n} f_i = \sum_{i=1}^{n} \frac{a_i \eta_i P_i^2}{\sum_{k=1}^{n} \eta_k P_k + \sum_{k=1}^{n} a_k h_k \eta_i P_k^2} \qquad \text{(A1)}$$

Now we split each species i into a group of m species with identical life traits, so that the values of a_i, h_i and η_i are the same within each group. For simplicity, we suggest that each species in group i has the same density $p_i = P_i/m$. Then we will have mn species in total. The overall intake rate is obtained by summing f_i over mn species:

$$f = \sum_{i=1}^{mn} f_i = \sum_{i=1}^{nm} \frac{a_i \eta_i p_i^2}{\sum_{k=1}^{nm} \eta_k p_k + \sum_{k=1}^{nm} a_k h_k \eta_i p_k^2}.$$

It is possible to show that

$$\sum_{k=1}^{nm} \eta_k p_k = \sum_{k=1}^{n} \eta_k P_k, \quad \sum_{k=1}^{nm} a_k h_k \eta_k p_k^2 = \frac{1}{m} \sum_{k=1}^{n} a_k h_k \eta_k P_k^2$$

and

$$\sum_{k=1}^{nm} a_k \eta_k p_k^2 = \frac{1}{m} \sum_{k=1}^{n} a_k \eta_k P_k^2.$$

Thus, for the total intake rate after splitting species into subgroups we have:

$$f = \sum_{i=1}^{mn} f_i = \frac{1}{m} \sum_{i=1}^{n} \frac{a_i \eta_i P_i^2}{\sum_{k=1}^{n} \eta_k P_k + \frac{1}{m} \sum_{k=1}^{n} a_k h_k \eta_i P_k^2} = \sum_{i=1}^{n} \frac{a_i \eta_i P_i^2}{m \sum_{k=1}^{n} \eta_k P_k + \sum_{k=1}^{n} a_k h_k \eta_i P_k^2} \qquad \text{(A2)}$$

The total intake rates (A1) and (A2) are different despite the fact that they describe consumption of the exactly same prey community. Moreover we find that

$$\sum_{i=1}^{n} \frac{a_i \eta_i P_i^2}{m\sum_{k=1}^{n} \eta_k P_k + \sum_{k=1}^{n} a_k h_k \eta_i P_k^2} < \sum_{i=1}^{n} \frac{a_i \eta_i P_i^2}{\sum_{k=1}^{n} \eta_k P_k + \sum_{k=1}^{n} a_k h_k \eta_i P_k^2}$$

Because the denominator in (A2) is greater than the denominator in (A1). Therefore, an increase in the number of species leads to a decrease of the overall intake rate.

Note that a similar discrepancy will also hold true if we add new species into the system, which leads to the redistribution the total prey biomass among a greater number of prey species.

Appendix 7. Using a different multi-prey functional response with imperfect selectivity

Along with the functional response defined by (1) and (4), we also investigated the consequences of other multi-prey functional responses with imperfect prey selectivity. In particular, we considered the functional response suggested by Morozov and Petrovskii (2013), given by

$$f_i = \frac{P_i \eta_i \sum_j \varepsilon_{ij} P_j}{\sum_i P_i \eta_i \sum_j \varepsilon_{ij} P_j} \cdot \frac{a_i \sum_j \eta_j P_j}{1 + h\sum_j a_j \eta_j P_j} \text{ . (A3)}$$

The coefficients ε_{ij} and η_i in (A3) have the same meaning as those in the main text of the paper and to be consistent with the simulations in the main text, we considered the same expression for the similarity coefficients ε_{ij} given by the exponential function (5). The biological rationale behind the response defined by (A3) is provided in (Morozov and Petrovskii, 2013). It meets the all consistency requirement suggested by Morozov and Petrovskii (2013). In particular, it can describe predation on species both with similar and distinctly different life traits. An important special feature of the response (A3) is that an increase of any prey density P_i always results in an elevated total food intake rate $\sum f_i$ (see rule v in Morozov and Petrovskii, 2013). Thus, this functional response avoids the so-called 'poisoning-effect'.

We have performed extensive numerical simulations of our food web model (6)-(8) with the functional response given by (A3), using the same way of introducing prey species into the system and the same trade-offs at the resource/prey level. These simulations have shown that the results obtained with (A3) are qualitatively similar to those described in the main text with the functional response (1) and (4). In particular, we found (i) predator-mediated coexistence of a large number of prey computing for a single resource with a similar shape of rank-abundance curves (see Fig. S5A); (ii) irregular biomass distributions across life traits of prey (see Fig. S5B); and (iii) a unimodal-like structure of the biodiversity curve as function of similarity parameter σ, both in terms of effective species numbers and functional biodiversity (not shown for the sake of brevity). The most notable difference is that for the same degree the degree of imperfectness σ the functional response (A3) generally allows the coexistence of more prey species than the response (1)-(4).

We obtained similar results also for different parameterizations of the functional response (1) and (4). For example, we have tested the scenario that the density-independent preferences η_i in (4) are not constant for all species, but are proportional to the attack rates, $\eta_i \sim a_i$. In this case our functional response becomes identical to the response by Leeuwen et al. (2013) for the special case that the handling times are independent from previously consumed prey ($T_{ij} = T_i$). Again, we obtained qualitatively the same model results.

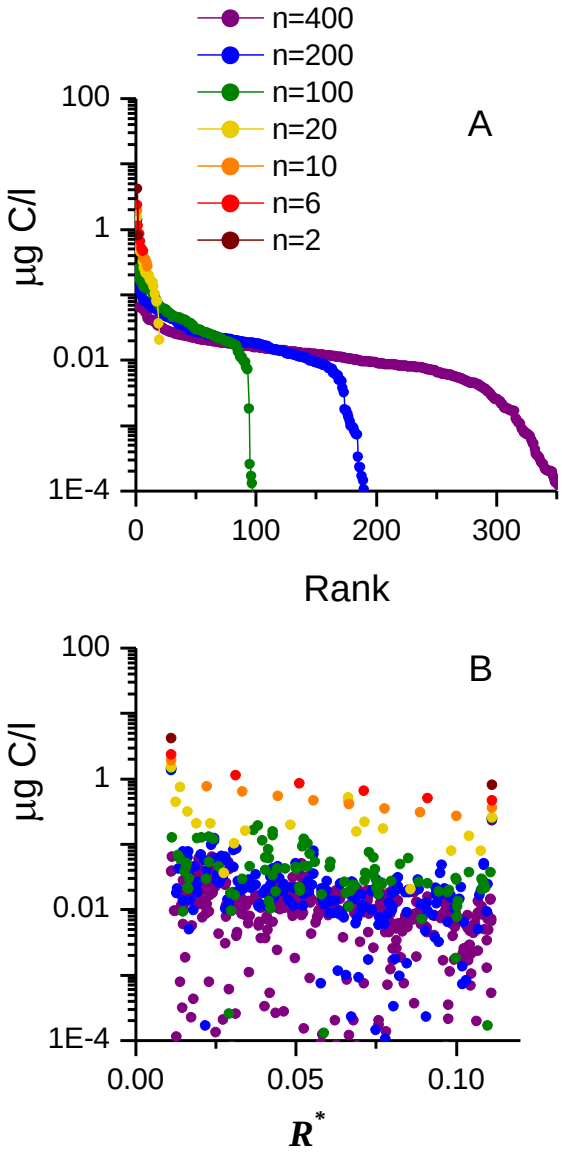

Fig. S5. Long-term density distributions of primary producers (P_i) in the food web model with the functional response of predator given by (A3) and (5). The figure shows the equilibrium density of each species sorted by species rank (i.e., the rank-abundance curve, top panel) and as a function of its R^* value (i.e., the trait-abundance curve, bottom panel). Different colors indicate the number n of species that have subsequently been introduced into the system (i.e., the number of invasion attempts). The imperfect prey selectivity parameter is $\sigma = 0.1$, the nutrient supply concentration is $N_0 = 5$. Other parameter values are the same as in Fig.1.

References

1. Agawin, N.S.R. Rabouille, S. Veldhuis, M.J.W. Van Overzee, H.M.J. Huisman, J. 2007. Competition and facilitation between unicellular nitrogen-fixing cyanobacteria and non–nitrogen-fixing phytoplankton species. *Limnol. Oceanogr.*, 52(5), 2233–2248
2. Botta-Dukát, Z. (2005). Rao's quadratic entropy as a measure of functional diversity based on multiple traits. *Journal of Vegetation Science*, 16, 533–540.
3. Edwards, A.M. & Brindley, J. 1996. Oscillatory behaviour in a three-component plankton population model. Dynamics and stability of Systems, 11, 347–370.
4. Edwards, K.F., Thomas, M.K., Klausmeier, C.A. & Litchman, E. (2012). Allometric scaling and taxonomic variation in nutrient utilization traits and maximum growth rate of phytoplankton. Limnol. Oceanogr, 57, 554–566.
5. Fukami, T. & Morin, P.J. (2003). Productivity–biodiversity relationships depend on the history of community assembly. Nature, 424, 423–426.
6. Kiørboe T. A, 2008. Mechanistic Approach to Plankton Ecology. Princeton University Press, NJ.
7. Morozov A., Arashkevich, E. Nikishina, A., Solovyev, K., 2011. Nutrient-rich plankton community stabilized via predator-prey interactions: revisiting the role of vertical heterogeneity. Math. Med. Biol., 28, 185–215.
8. Pielou, E.C. (1966). The Measurement of Diversity in Different Types of Biological Colledions. J. Theor. Biol., 13, 131–144.
9. Pigolotti, S., C. López, and E. Hernández-García.(2007) Species clustering in competitive Lotka-Volterra Models. *PRL* 98, 258101.
10. Pomati F., Jokela J., Simona M., Veronesi M., Ibelings B.W. (2011). An automated platform for phytoplankton ecology and aquatic ecosystem monitoring. Environmental Science and Technology 45 (22), 9658–9665.
11. Redfield, A.C. (1958). The biological control of chemical factors in the environment. American scientist, 230A–221.
12. Schwaderer, A.S., Yoshiyama, K., de Tezanos Pinto, P., Swenson, N.G., Klausmeier, C.A. & Litchman, E. (2011). Eco-evolutionary differences in light utilization traits and distributions of freshwater phytoplankton. Limnol. Oceangr., 56, 589–598.
13. Sunda, W.G., Shertzer, K.W., Hardison, D.R., 2009. Ammonium uptake and growth models in marine diatoms: Monod and Droop revisited. Marine Ecology Progress Series, 386, 29–41.